JOURNAL OF COMPUTATIONAL PHYSICS 80, 288–313 (1989)

A Nonconforming Combination for Solving Elliptic Problems with Interfaces

ZI-CAI LI

Centre de Recherche Informatique de Montréal Inc., 1550, de Maisonneuve Blvd West, Montréal, Québec, Canada H3G 1N2, and Department of Computer Science, Concordia University, Montréal, Québec, Canada H3G 1M8

Received June 18, 1987; revised November 30, 1987

Nonconforming combinations are provided for solving interface problems of elliptic equations. In these approaches, the Ritz–Galerkin method with particular solutions is used for the part of a solution domain where there are interface singular points; and the conventional finite element method is used for the rest of the solution domain. In addition, admissible functions chosen are constrained to be continuous only at the element nodes on the common boundary of the subdomains. Error bounds are derived in the Sobolev norms, and numerical experiments are given for solving a model interface problem of the equation, $-\Delta u + u = 0$. Moreover, a significant coupling relation, $L+1 = O(|\ln h|)$, is found for interface problems by using the nonconforming combinations, where $(L+1)$ is the total number of particular solutions used in the Ritz–Galerkin method, and h is the maximal boundary length of triangular elements in the finite element method.

1. INTRODUCTION

Efficient numerical methods for the solution of mathematical and physical problems with singularities are significant because the conventional finite element method and finite difference method fail to deal with them. For angular singularity problems, there have appeared the conformal transformation methods of Whiteman and Papmichael [21], the infinite grid refinement method of Thatcher [20] and Gregory *et al.* [8], and the coupling method of the boundary and element methods of Zienkiewicz *et al.* [26]. But the most promising approaches are those that use the singular functions near singular points. In fact, Fix *et al.* [7] and Strang and Fix [19] provide an innovative method by adding the singular functions into piecewise interpolation polynomials in the standard finite element methods, but Wigley [23, 24] present an inverse approach by subtracting singular expansions from the solutions obtained by the finite element methods. Our question, however, is: should we use only the singular functions in the neighbourhood of the singular points? Certainly we should. In fact, the idea that uses only the singular functions in a subdomain can be easily performed in the nonconforming combined methods

0021-9991/89 $3.00

[13–15] as long as the singular functions have been known. In the subdomains including angular singular points, only particular solutions (singular or analytic) are used; in other subdomains without singularities, the conventional finite element methods are still used as usual. Since a nonconforming strategy is employed for matching the Ritz–Galerkin method and the finite element method, the nonconforming combination is referred to. In this paper the Ritz–Galerkin method is referred to if a subspace of particular solutions is used, and the finite element method if a subspace of piecewise linear functions is used. Besides the combined approaches, other treatments can be also found in Zielinski and Zienkiewicz [25], Li [15], and Li *et al.* [16] where piecewise singular and analytic functions are applied to whole solution domains, instead of the finite element method completely. In this paper, we will focus on interface problems only by the nonconforming combinations and will provide some new numerical techniques. For the interface problems of elliptic equations, Kellogg [10–12] and Babuška [1] provide a theoretical base for their singularity property (also see Birkhoff [4] and Strang and Fix [19]). The singularity at the corners of interfaces will reduce the precision of numerical solutions by the traditional finite element method or finite difference method. Hence, Han [9] presents the infinite element method which yields a satisfactory numerical solution for interface problems of the Laplace equation. But the method of Han cannot be applied to other elliptic equations, such as

$$-\Delta u + u = 0. \tag{1.1}$$

We now introduce the nonconforming combinations for Eq. (1.1) which consists of three steps as follows:

1. Suppose that there exists only one singular point of interfaces. The solution domain is then divided into two subdomains. One of them includes the singular point, and it is called the singular subdomain.

2. On the singular subdomain, the Ritz–Galerkin method is used with particular solutions of interface problems as admissible functions. On the other subdomain the finite element method is used with piecewise linear interpolation functions as admissible functions. We notice that when the intersection angles of the interfaces are $\Theta = \pi/n$, $n = 2, 3, \ldots$, some analytic eigenfunctions have to be added to Kellogg's singular eigenfunctions, in order to form a complete set of eigenfunctions (Li [15]).

In addition, these admissible functions are constrained to be continuous only at the element nodes on the common boundary of two subdomains where two different methods (i.e., the Ritz–Galerkin method and the finite element method) are used simultaneously. This approach is nonconforming because the admissible functions are not continuous on the whole common boundary.

3. Finally, a system of algebraic equations can be obtained. Since its coefficient matrix is positive definite and symmetric, the numerical solutions of the combinations are easily solved.

We shall provide error bounds of numerical solutions. Based on error analyses, a significant coupling relation such as that of Li [14]:

$$L+1=O(|\ln h|). \tag{1.2}$$

is also proved for interface problems of (1.1), where $(L+1)$ is the total number of particular solutions in the singular domain, and h is the largest boundary length of triangular elements used in the finite element method.

Numerical experiments using coupling relation (1.2) are carried out for a model problem of interfaces. In fact, only six terms of particular solutions are required for a good approximate solution. In summary, both theoretical analyses and numerical results in this paper will again show outstanding advantages of the nonconforming methods in solving interface problems provided that the asymptotic expansions of true solutions near the interface singularities can be found.

2. Interface Problem

Consider the interface problem of two dimensions (Fig. 1):

$$p^+(-\Delta u+u)=0, \qquad \text{in } \Omega^+, \tag{2.1a}$$

$$p^-(-\Delta u+u)=0, \qquad \text{in } \Omega^-, \tag{2.1b}$$

$$u^+=u^-, \qquad p^+\frac{\partial u^+}{\partial n}=p^-\frac{\partial u^-}{\partial n} \qquad \text{on } \bar{\Gamma}_0, \tag{2.1c}$$

$$u=g(x,y), \qquad \text{on } \partial\Omega, \tag{2.1d}$$

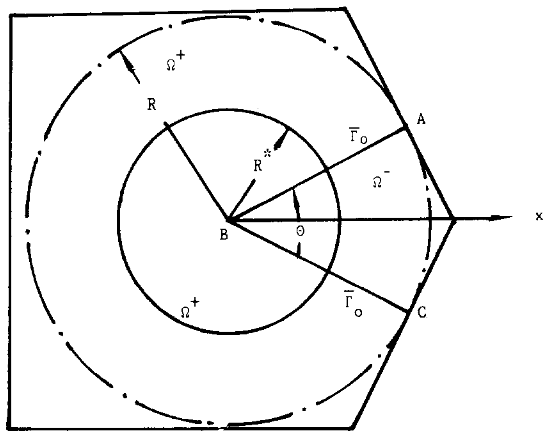

Fig. 1. An interface problem.

where $\Delta = \partial^2/\partial x^2 + \partial^2/\partial y^2$, the solution domain Ω $(=\Omega^+ \cup \Omega^-)$ is a convex polygon, the interface boundary $\bar{\Gamma}_0$ $(=\Omega^+ \cap \Omega^-)$ is made up of the piecewise straight lines ABC, with an intersection angle Θ, n is the normal to $\bar{\Gamma}_0$, $u^\pm = u|_{\Omega^\pm}$, $p^\pm$ are positive constants, and the function $g(x, y)$ is a sufficiently smooth function on $\partial\Omega$.

The solutions near the interface singularity B have expansions:

$$u(r, \theta) = \sum_{i=0}^{\infty} D_i I_{\mu_i}(r)\, \phi_{\mu_i}(\theta), \tag{2.2}$$

where $\mu_i \leqslant \mu_{i+1}$, D_i are expansion coefficients, $I_\mu(r)$ are the Bessel functions for a purely imaginary argument, defined by (Watson [22])

$$I_\mu(r) = \sum_{k=0}^{\infty} \frac{1}{\Gamma(k+1)\Gamma(k+\mu+1)} \left(\frac{r}{2}\right)^{2k+\mu} \tag{2.3a}$$

or

$$I_\mu(r) = \frac{(\frac{1}{2}r)^\mu}{\Gamma(\frac{1}{2})\Gamma(\mu+\frac{1}{2})} \int_{-1}^{1} e^{\pm rt}(1-t^2)^{\mu-1/2}\, dt, \tag{2.3b}$$

and $\phi_{\mu_i}(\theta)$ are complete orthogonal eigenfunctions of a Sturm–Liouville system, which fall into symmetric and anti-symmetric groups.

Kellogg [10–12] provides two groups of eigenfunctions.

1. *Symmetric eigenfunctions*:

$$\phi_{\hat{\mu}_j}(\theta) = \begin{cases} \cos \hat{\mu}_j \theta, & |\theta| < \Theta/2, \\ \hat{\alpha}_j \cos \hat{\mu}_j(\pi - \theta), & |\theta| > \Theta/2, \end{cases} \tag{2.4}$$

where the constants are

$$\hat{\alpha}_j = \cos \hat{\mu}_j \frac{\Theta}{2} \Big/ \cos \hat{\mu}_j \left(\pi - \frac{\Theta}{2}\right), \tag{2.5}$$

and $\hat{\mu}_j$ satisfy the equations

$$p^- \operatorname{tg} \hat{\mu}_j \frac{\Theta}{2} + p^+ \operatorname{tg} \hat{\mu}_j \left(\pi - \frac{\Theta}{2}\right) = 0. \tag{2.6}$$

2. *Antisymmetric eigenfunctions*:

$$\phi \bar{\mu}_j(\theta) = \begin{cases} \sin \bar{\mu}_j \theta, & |\theta| < \Theta/2, \\ \bar{\alpha}_j \sin \bar{\mu}_j(\pi - \theta), & |\theta| > \Theta/2, \end{cases} \tag{2.7}$$

where the constants are

$$\bar{\alpha}_j = \sin \bar{\mu}_j \frac{\Theta}{2} \Big/ \sin \bar{\mu}_j \left(\pi - \frac{\Theta}{2}\right), \tag{2.8}$$

and $\bar{\mu}_j$ satisfy

$$p^+ \operatorname{tg} \bar{\mu}_j \frac{\Theta}{2} + p^- \operatorname{tg} \bar{\mu}_j \left(\pi - \frac{\Theta}{2}\right) = 0. \tag{2.9}$$

When the intersection angles of interfaces are

$$\Theta = \pi/n, \qquad n = 2, 3, ,..., \tag{2.10}$$

some additional eigenfunctions have to be added to Kellogg's eigenfunctions of the Sturm–Liouville system so that a complete set of eigenfunctions is formed. These additional eigenfunctions are [15]:

1. *Symmetric eigenfunctions*:

$$\phi_{2nk}(\theta) = \cos 2nk\theta, \qquad 0 \leqslant \theta \leqslant \pi, \tag{2.11}$$

and

$$\phi_{n(2k+1)}(\theta) = \begin{cases} \cos n(2k+1)\theta, & |\theta| < \Theta/2 = \pi/2n, \\ (p^-/p^+) \cos n(2k+1)\theta, & |\theta| > \Theta/2 = \pi/2n, \end{cases} \tag{2.12}$$

where $k = 0, 1, \ldots$.

2. *Antisymmetric eigenfunctions*:

$$\phi_{2nk}(\theta) = \begin{cases} \sin 2nk\theta, & |\theta| < \Theta/2 = \pi/2n, \\ (p^-/p^+) \cos 2nk\theta, & |\theta| > \Theta/2 = \pi/2n, \end{cases} \tag{2.13}$$

and

$$\phi_{n(2k-1)}(\theta) = \sin n(2k-1)\theta, \qquad 0 \leqslant \theta \leqslant \pi, \tag{2.14}$$

where $k = 1, 2, \ldots$.

A typical interface problem as in Fig. 2 has been discussed in Strang and Fix [19], where the solution domain is a square domain $(-1 < x < 1,\ -1 < y < 1)$, and Ω^- is a small square domain $(-\frac{1}{2} < x < \frac{1}{2},\ -\frac{1}{2} < y < \frac{1}{2})$. There then exist four singular points of interfaces with the intersection angles

$$\Theta = \pi/2, \tag{2.15}$$

i.e., $n = 2$ for $\Theta = \pi/n$. In this case, corresponding complete eigenfunctions are:

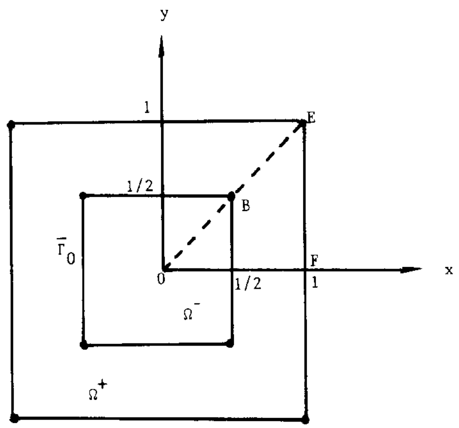

FIG. 2. An interface problem on the solution domain Ω.

1. *Symmetric eigenfunctions*: Kellogg's functions (2.4) with the constants $\hat{\alpha}_j$, (2.5), and

$$\hat{\mu}_{4j\pm 1} = 4j \pm \alpha^* \tag{2.16}$$

where

$$\alpha^* = \frac{4}{\pi} \operatorname{arctg} \sqrt{\frac{3 + p^-/p^+}{1 + 3p^-/p^+}}, \tag{2.17}$$

as well as the additional functions

$$\phi_{4k}(\theta) = \cos 4k\theta, \qquad 0 \leqslant \theta \leqslant \pi, \tag{2.18}$$

and

$$\phi_{2(2k+1)}(\theta) = \begin{cases} \cos 2(2k+1)\theta, & |\theta| < \pi/4, \\ (p^-/p^+) \cos 2(2k+1)\theta, & |\theta| > \pi/4, \end{cases} \tag{2.19}$$

where $k = 0, 1, \ldots$.

2. *Antisymmetric eigenfunctions*: Kellogg's functions (2.7) with the constants $\bar{\alpha}_j$, (2.8), and

$$\bar{\mu}_{(4j+2)\pm 1} = 4j + 2 \pm \alpha^*, \tag{2.20}$$

as well as the additional functions

$$\phi_{4k}(\theta) = \begin{cases} \sin 4k\theta, & |\theta| < \pi/4, \\ (p^-/p^+) \sin 4k\theta, & |\theta| > \pi/4, \end{cases} \tag{2.21}$$

and

$$\phi_{2(2k-1)}(\theta) = \sin 2(2k-1)\theta, \qquad 0 \leqslant \theta \leqslant \pi,$$

where $k = 1, 2, \ldots$.

Now, denote the minimal nonzero eigenvalue $\mu_{\min}$ as

$$\mu_{\min} = \min_{\mu_i > 0} \mu_i. \tag{2.22}$$

Then, when $\Theta = \pi/2$,

$$\mu_{\min} = \min[\alpha^*, 2 - \alpha^*], \tag{2.23}$$

where α^* is defined by (2.17), and also when $p^+ \neq p^-$,

$$\tfrac{2}{3} < \mu_{\min} < 1. \tag{2.24}$$

Moreover, for the symmetric cases with $\mu_{\min} = \alpha^*$, Ineq. (2.24) holds true if and only if

$$p^+ < p^-. \tag{2.25}$$

In fact, the main part of singular expansions of u near the singularity B is

$$u = O(I_{\mu_{\min}}(r)). \tag{2.26}$$

On the other hand, we have from (2.3b)

$$I_{\mu_{\min}}(r) \leqslant \alpha_{\mu_{\min}} e^r r^{\mu_{\min}} \tag{2.27}$$

with a constant

$$\alpha_\mu = \frac{(\frac{1}{2})^\mu}{\Gamma(\frac{1}{2})\Gamma(\mu + \frac{1}{2})} \int_{-1}^{1} (1 - t^2)^{\mu - 1/2}\, dt. \tag{2.28}$$

Hence $u = O(r^{\mu_{\min}})$. Also for (2.24), the derivatives have

$$\left|\frac{\partial u}{\partial r}\right| = O(r^{\mu_{\min} - 1}) \to \infty \qquad \text{as} \quad r \to 0.$$

This shows the singularity property of solutions near the singular point B for interface problem (2.1).

In practical application, we prefer the solution expansions with scale factors:

$$u = \sum_{i=0}^{\infty} D_i \frac{I_{\mu_i}(r)}{I_{\mu_i}(R)} \phi_{\mu_i}(\theta), \qquad 0 \leqslant r \leqslant R \quad \text{and} \quad 0 \leqslant \theta \leqslant \pi, \tag{2.29}$$

to (2.2), where R is a radius, which may be chosen as the inscribed radius of Ω shown in Fig. 1. Clearly, when $r=R$, the solution is

$$u(R, \theta)=\sum_{i=0}^{\infty} D_i \phi_{\mu_i}(\theta), \qquad 0 \leqslant \theta \leqslant \pi. \tag{2.30}$$

Then the coefficients D_i can be represented from the orthogonality of eigenfunctions $\phi_{\mu_i}(\theta)$:

$$D_i=\frac{\int_0^{2\pi} pu(R, \theta)\, \phi_{\mu_i}(\theta)\, d\theta}{\int_0^{2\pi} p\phi_{\mu_i}^2(\theta)\, d\theta}, \tag{2.31}$$

where the function is

$$p=\begin{cases} p^-, & |\theta|<\Theta/2, \\ p^+, & |\theta|>\Theta/2. \end{cases} \tag{2.32}$$

3. Nonconforming Combinations

We shall use the nonconforming combination of the Ritz–Galerkin and finite element methods for solving the interface problem (2.1).

Divide the solution domain Ω of Fig. 3 into Ω_1 and Ω_2 by a circle l_{R^*} ($r=R^*$). Let Ω_2 be the disk: $r<R^*$ and $0 \leqslant \theta \leqslant 2\pi$, and Ω_1 the rest of Ω. We notice that the common boundary l_{R^*} is not the interface boundary $\bar{\Gamma}_0$.

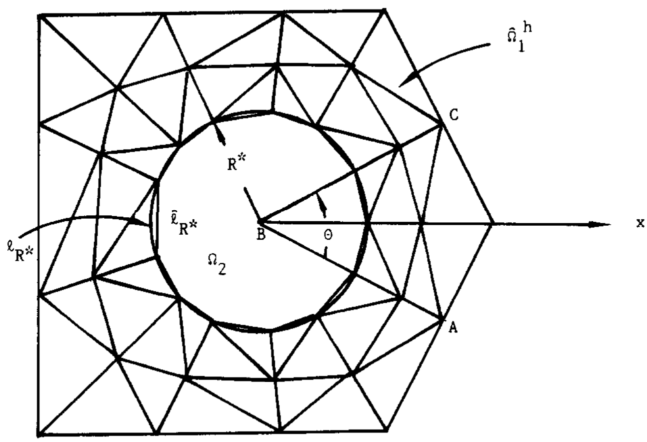

FIG. 3. A division of the solution domain.

Since $u \in H^2(\Omega_1)$ but $u \notin H^2(\Omega_2)$ for $p^+ \neq p^-$, we use the finite element method with a subspace of piecewise linear functions in Ω_1 and the Ritz–Galerkin method with a subspace of particular solutions in Ω_2 for the interface problem. In fact, the subdomain Ω_1 is again divided into many small triangle elements Δ_i (see Fig. 3). Let $\hat{\Omega}_1^h = \bigcup_i \Delta_i$, then $\hat{\Omega}_1^h \approx \Omega_1$. Also $\hat{\Omega}_1^h$ extends partly into Ω_2 so that there is a small overlap region of $\hat{\Omega}_1^h$ and Ω_2, i.e., Area $(\hat{\Omega}_1^h \cap \Omega_2) \neq 0$. The theoretical analysis in [13–15] shows that such an overlap does not cause a reduced convergence rate of numerical solutions. Therefore we do not need to use the complicated, isoparametric elements in coupling two kinds of subspaces along a curved common boundary l_{R^*}.

Based on (2.29) admissible functions can be chosen as

$$v = \begin{cases} \bar{v}^{(1)} \text{ satisfying (2.1d)}, & \text{in } \hat{\Omega}_1^h, \\ v_L = \sum_{i=0}^{L} (\tilde{D}_i \, I_{\mu_i}(r)/I_{\mu_i}(R)) \, \phi_{\mu_i}(\theta), & \text{in } \Omega_2, \end{cases} \tag{3.1}$$

where $\bar{v}_1^{(1)}$ are piecewise linear interpolation polynomials on the triangulation domain $\hat{\Omega}_1^h$ of Ω_1, and $\tilde{D}_i$ are coefficients to be calculated. Note that $\bar{v}^{(1)}$ in (3.1) can satisfy (2.1d) exactly if $g(x, y)$ is a linear function with respect to x and y; otherwise, similar error analysis can be found in Strang and Fix [19].

In addition, the admissible functions v in (3.1) are also required to satisfy the continuity conditions at the element nodes $P_j(R^*, \theta_j)$ on the common boundary l_{R^*} $(r = R^*)$:

$$\bar{v}^{(1)}(R^*, \theta_j) = \sum_{i=0}^{L} \tilde{D}_i \frac{I_{\mu_i}(R^*)}{I_{\mu_i}(R)} \phi_{\mu_i}(\theta_j), \qquad \forall P_j \qquad \text{on } l_{R^*}. \tag{3.2}$$

It is noted from (3.2) that this approach is nonconforming because the admissible functions chosen are not continuous on the whole common boundary l_{R^*}.

Now, we give the definitions of the function spaces V_h^0 and V_h. Let V_h denote the space of v in (3.1) with the constraint conditions (3.2), and V_h^0 denote the space of the functions

$$w = \begin{cases} \bar{v}^{(1)} & \text{but satisfying } \bar{v}^{(1)}|_{\partial\Omega} = 0, \\ v_L, \end{cases} \tag{3.3}$$

with (3.2).

Therefore, the combination of the Ritz–Galerkin and finite element methods is designed to find an approximate solution $u_h^* \in V_h$ such that

$$B_h(u_h^*, v) = 0, \qquad \forall v \in V_h^0, \tag{3.4}$$

where the bilinear form is

$$B_h(u, v) = \iint_{\Omega_2 \cap \Omega^+} p^+(u_x v_x + u_y v_y + uv)\, d\Omega$$

$$+ \iint_{\Omega_2 \cap \Omega^-} p^-(u_x v_x + u_y v_y + uv)\, d\Omega$$

$$+ \iint_{\hat{\Omega}_1^h \cap \Omega^+} p^+(u_x v_x + u_y v_y + uv)\, d\Omega$$

$$+ \iint_{\hat{\Omega}_1^h \cap \Omega^-} p^-(u_x v_x + u_y v_y + uv)\, d\Omega, \tag{3.5}$$

where Ω^+ and Ω^- are defined in Eqs. (2.1) shown in Fig. 1.

After elimination of the unknown $\bar{v}^{(1)}(R^*, \theta_j)$ in (3.4) by the constraints (3.2), we obtain a linear system of algebraic equations

$$Tx = b, \tag{3.6}$$

where x is the unknown vector with the components $\tilde{D}_i$ and $\bar{v}^{(1)}(r_i, \theta_j)$ $(r_i > R^*)$, b is a known vector, and the coefficient matrix T is positive definite, symmetric, and sparse. Consequently, the solutions x (i.e., u_h^*) in (3.6) can be easily solved by the direct methods in Birkhoff and Lynch [5].

4. Error Estimates and Coupling Strategy

Define a norm over V_h^0:

$$\|v\|_h = (\|v\|^2_{1,\hat{\Omega}_1^h} + \|v\|^2_{1,\Omega_2})^{1/2}, \tag{4.1}$$

where $\|\cdot\|_{m,\Omega_2}$ is the Sobolev norm [18]. Then we have by following the work of [14, 15]:

Theorem 1. *Let*

$$R^* < R \tag{4.2}$$

and

$$u \in H^2(\Omega_1), \tag{4.3}$$

and suppose that the family of triangular elements with the maximal boundary length h in $\hat{\Omega}_1^h$ is quasi-uniform. Then there exists a bounded constant C independent of h, L, and u such that

$$\|u - u_h^*\|_h \leqslant C\{h + \|\mathbf{R}_L\|_{1,\hat{\Omega}_2} + \mu_L^2 h^2\}, \tag{4.4}$$

where $\tilde{\Omega}_2$ *is a disk* $(r \leqslant R_2)$ *with*

$$R^* < R_2 < R, \tag{4.5}$$

the remainder R_L *is*

$$R_L = \sum_{i=L+1}^{\infty} D_i \frac{I_{\mu_i}(r)}{I_{\mu_i}(R)} \phi_{\mu_i}(\theta) \tag{4.6}$$

with the expansion coefficients D_i *defined by* (2.31).

Below, we shall further estimate bounds of $\|\mathbf{R}_L\|_{1,\tilde{\Omega}_2}$.

LEMMA 1. *There exists a bounded constant C independent of* μ *such that*

$$\frac{I_\mu(r)}{I_\mu(R)} \leqslant C\left(\frac{r}{R}\right)^\mu, \qquad \forall \mu > 0. \tag{4.7}$$

Proof. We have from (2.3b)

$$\alpha_\mu e^{-r} r^\mu \leqslant I_\mu(r) \leqslant \alpha_\mu e^r r^\mu,$$

with the constant α_μ defined by (2.28). It then follows that

$$\frac{I_\mu(r)}{I_\mu(R)} \leqslant e^{(R+r)}\left(\frac{r}{R}\right)^\mu = C\left(\frac{r}{R}\right)^\mu$$

with $C = e^{(R+r)}$. This completes the proof of Lemma 1.

LEMMA 2. *Let* (4.3) *hold, there then exists a constant C independent of* μ_i *such that*

$$|D_i| \leqslant C/\mu_i$$

for all $\mu_i > 0$, *where the coefficients* D_i *are defined by* (2.31).

Proof. The eigenfunctions $\phi_{\mu_i}(\theta)$ of the Sturm–Liouville system discussed in Section 2 are complete and orthogonal:

$$\int_0^{2\pi} p\phi_{\mu_i}(\theta)\, \phi_{\mu_j}(\theta)\, d\theta = \begin{cases} 0, & i \neq j, \\ \beta_i, & i = j, \end{cases} \tag{4.8}$$

where β_i are positive constants such that

$$\beta_i \leqslant C < \infty. \tag{4.9}$$

Define the functions

$$p = \begin{cases} p^-, & |\theta| < \Theta/2, \\ p^+, & |\theta| > \Theta/2, \end{cases} \tag{4.10}$$

$$\psi_{\mu_i}(\theta) = -\frac{1}{\mu_i}\frac{d}{d\theta}\phi_{\mu_i}(\theta), \tag{4.11}$$

where $\phi_{\mu_i}(\theta)$ are the eigenfunctions of the Sturm–Liouville system. Since

$$\frac{d^2\phi_{\mu_i}(\theta)}{d\theta^2} = -\mu_i^2 \phi_{\mu_i}(\theta), \tag{4.12}$$

we have

$$\frac{1}{\mu_i}\frac{d}{d\theta}\psi_{\mu_i} = \phi_{\mu_i}(\theta). \tag{4.13}$$

By noting (2.31), (4.11), and (4.13), and the condition $\mu_i > 0$, we obtain from integration by parts

$$\begin{aligned} D_i &= \frac{1}{\beta_i}\int_0^{2\pi} pu(R,\theta)\,\phi_{\mu_i}(\theta)\,d\theta \\ &= \frac{1}{\beta_i\mu_i}\int_0^{2\pi} pu(R,\theta)\,d\psi_{\mu_i}(\theta)\,d\theta \\ &= -\frac{1}{\beta_i}\left\{u\left(R,\frac{\Theta}{2}\right)\left[p^+\frac{d}{d\theta}\phi_{\mu_i}\left(\frac{\Theta}{2}+0\right)\right.\right. \\ &\quad \left. -p^-\frac{d}{d\theta}\phi_{\mu_i}\left(\frac{\Theta}{2}-0\right)\right] + u\left(R,\frac{\Theta}{2}\right) \\ &\quad \left.\times\left[p^-\frac{d}{d\theta}\phi_{\mu_i}\left(-\frac{\Theta}{2}+0\right) - p^+\frac{d}{d\theta}\phi_{\mu_i}\left(-\frac{\Theta}{2}-0\right)\right]\right\} \\ &\quad -\frac{1}{\beta_i\mu_i}\int_0^{2\pi} p\frac{\partial u}{\partial\theta}(R,\theta)\,\psi_{\mu_i}(\theta)\,d\theta. \end{aligned} \tag{4.14}$$

Because the eigenfunctions $\phi_{\mu_i}(\theta)$ satisfy the normal flux continuity condition across the interfaces (see (2.1c)), the coefficients are reduced to

$$D_i = -\frac{1}{\beta_i\mu_i}\int_0^{2\pi} p\frac{\partial u}{\partial\theta}(R,\theta)\,\psi_{\mu_i}(\theta)\,d\theta. \tag{4.15}$$

Therefore, using the Sobolev imbedding theorem and assumption (4.3) gives

$$|D_i| \leqslant \frac{C}{\mu_i}|u|_{1,l_R} \leqslant \frac{C'}{\mu_i}\|u\|_{2,\Omega_1} \leqslant \frac{C''}{\mu_i}, \tag{4.16}$$

with the bounded constants C, C', and C'', independent of μ_i (>0). This completes the proof of Lemma 2.

LEMMA 3. *When the conditions in Theorem* 1 *hold true, then*

$$\|\mathbf{R}_L\|_{1,\tilde{\Omega}_2} \leqslant \frac{C}{\sqrt{\mu_{L+1}}}\left(\frac{R_2}{R}\right)^{\mu_{L+1}}. \tag{4.17}$$

Proof. The family of $\psi_{\mu_i}(\theta)$ defined by (4.11) are also orthogonal:

$$\int_0^{2\pi} p\psi_{\mu_i}(\theta)\,\psi_{\mu_j}(\theta)\,d\theta=\int_0^{2\pi} p\phi_{\mu_i}(\theta)\,\phi_{\mu_j}(\theta)\,d\theta=\begin{cases}0, & i\neq j,\\ \beta_i, & i=j.\end{cases} \tag{4.18}$$

As a result of this orthogonality, we have

$$\begin{aligned}\|\mathbf{R}_L\|^2_{1,\tilde{\Omega}_2}&=\int_0^{2\pi}\int_0^{R_2}\left[\left(\frac{\partial \mathbf{R}_L}{\partial r}\right)^2+\left(\frac{\partial \mathbf{R}_L}{r\,\partial\theta}\right)^2+\mathbf{R}_L^2\right] r\,dr\,d\theta\\ &=\sum_{i=L+1}^{\infty} D_i^2\beta_i^2\int_0^{R_2}\left\{\frac{[I'_{\mu_i}(r)]^2+[1+(\mu_i/r)^2]\,I^2_{\mu_i}(r)}{I^2_{\mu_i}(R)}\right\} r\,dr. \end{aligned}\tag{4.19}$$

Since the bounds of $I'_{\mu_i}(r)$ can be found from (2.3b):

$$I'_\mu(r)\leqslant\left(\frac{\mu}{r}+1\right)I_\mu(r), \tag{4.20}$$

we obtain the integration bounds by Lemma 1:

$$\int_0^{R_2}\left\{\frac{[I'_{\mu_i}(r)]^2+[1+(\mu_i/r)^2]\,I^2_{\mu_i}(r)}{I^2_{\mu_i}(R)}\right\} r\,dr\leqslant C\mu_i\left(\frac{R_2}{R}\right)^{2\mu_i}. \tag{4.21}$$

Consequently, we have from Lemma 2 and bounded constants β_i

$$\begin{aligned}\|\mathbf{R}_L\|^2_{1,\tilde{\Omega}_2}&\leqslant C\sum_{i=L+1}^{\infty}\frac{1}{\mu_i}\left(\frac{R_2}{R}\right)^{2\mu_i}\\ &\leqslant C\frac{1}{\mu_{L+1}}\left(\frac{R_2}{R}\right)^{2\mu_{L+1}}\sum_{i=L+1}^{\infty}\left(\frac{R_2}{R}\right)^{2(\mu_i-\mu_{L+1})}.\end{aligned}\tag{4.22}$$

The eigenvalues μ_i of the Sturm–Liouville system satisfy

$$\delta_{\min}=\min_{\mu_i\neq\mu_j}|\mu_i-\mu_j|\geqslant\delta>0, \tag{4.23}$$

where δ is a constant independent of i. Also the eigenvalues, corresponding symmetric (or antisymmetric) eigenfunctions, differ from each other. Then

$$\|\mathbf{R}_L\|^2_{1,\tilde{\Omega}_2}\leqslant\frac{C}{\mu_{L+1}}\left(\frac{R_2}{R}\right)^{2\mu_{L+1}}\sum_{i=L+1}^{\infty}a_0^i, \tag{4.24}$$

where the constants $a_0=(R_2/R)^{2\delta_{\min}}$. Noting assumption (4.2) and $R^*<R_2<R$, then the constant $a_0<1$. The desired result (4.17) is obtained; this completes the proof of Lemma 3.

From Theorem 1 and Lemma 3, we have

THEOREM 2. *Let all conditions in Theorem 1 hold true, then*

$$\|u-u_h^*\|_h \leqslant C\left\{h+\frac{1}{\sqrt{\mu_{L+1}}}\left(\frac{R_2}{R}\right)^{\mu_{L+1}}+\mu_L^2 h^2\right\}. \tag{4.25}$$

Assume that all eigenvalues μ_n satisfy

$$\mu_n \leqslant C^* n+\bar{C}, \tag{4.26}$$

where the positive constants C^* and $\bar{C}$ are independent of n. Then the error bounds (4.25) become

$$\|u-u_h^*\|_h \leqslant C\left\{h+\left(\frac{R_2}{R}\right)^{C^*(L+1)}+L^2 h^2\right\}. \tag{4.27}$$

Clearly, when

$$\left(\frac{R_2}{R}\right)^{C^*(L+1)}=Ch, \tag{4.28}$$

we have

$$\|u-u_h^*\|_h \leqslant Ch. \tag{4.29}$$

This important conclusion is now written in a corollary:

COROLLARY. *Suppose that* (4.26) *and all conditions in Theorem* 1 *hold true. Then there exist error bounds* (4.29) *provided that* Eq. (4.28) *is satisfied.*

Equation (4.28) gives the coupling relation between $L+1$ and h:

$$L+1=\frac{\ln C+\ln h}{C^* \ln(R_2/R)}. \tag{4.30}$$

While $h \to 0$, we have a significant asymptotic relation

$$L+1=O(|\ln h|). \tag{4.31}$$

A useful formula is also derived from (4.30):

$$L_{h'}+1=(L_h+1)+\frac{|\ln(h'/h)|}{C^*|\ln(R_2/R)|}, \tag{4.32}$$

where the notation is

$$L_h+1=\frac{\ln C+\ln h}{C^* \ln(R_2/R)}, \tag{4.33}$$

with respect to a fixed h. Therefore, if a suitable total number L_h+1 of particular solutions used has been known, we may anticipate, directly from (4.32), another suitable total number $L_{h'}+1$ for a new triangulation with a smaller h' ($<h$).

Take Fig. 2 as an example where $\Theta=\pi/2$. It follows from (2.16) to (2.20) that

$$\mu_n \leqslant n, \tag{4.34}$$

i.e., $C^*=1$ in assumption (4.26). Then coupling relations (4.30) and (4.32) yield

$$L+1=\frac{\ln C+\ln h}{\ln(R_2/R)}. \tag{4.35}$$

and

$$L_{h'}+1=(L_h+1)+\frac{|\ln(h'/h)|}{|\ln(R_2/R)|}. \tag{4.36}$$

In particular, let $R=\frac{1}{2}$ and $R^*=\frac{1}{4}$, i.e., $R^*=R/2$. While $R_2 \to R^*$, we obtain from (4.36)

$$L_{h/2}+1 \approx (L_h+1)+1. \tag{4.37}$$

This means that only, almost, one more particular solution in Ω_2 is required when all boundary lengths of triangular elements in Ω_1 proportionally decrease to their halves. This clearly shows great advantages of the coupling strategy stated above.

5. Numerical Experiments

We consider the model problem (2.1) only on the solution domain as Fig. 2 with the exterior boundary condition

$$u=1 \qquad \text{on } \partial\Omega. \tag{5.1}$$

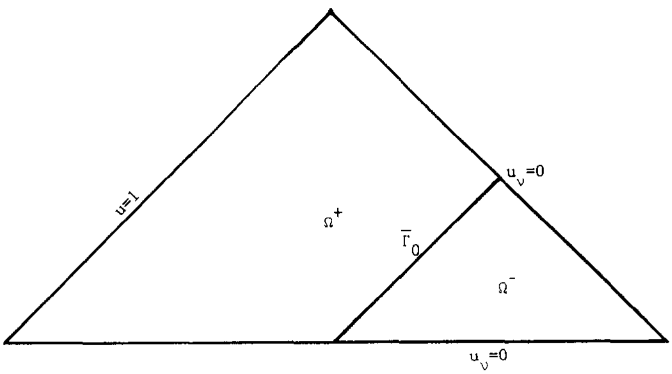

Fig. 4. One eighth of the solution domain in Fig. 2.

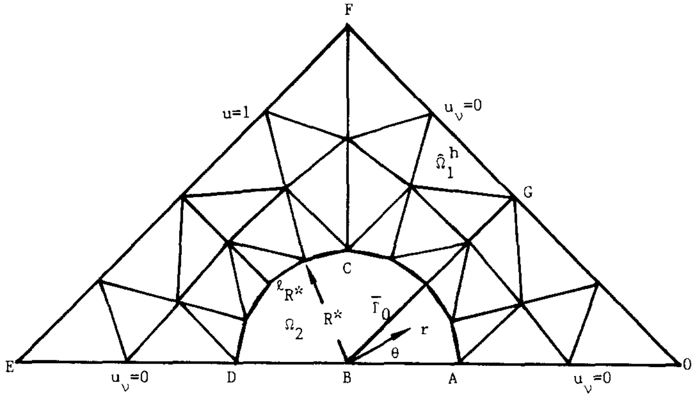

FIG. 5. A division on one eighth of the solution domain Ω for the combined method.

Because of the model's symmetry, it suffices to solve one eighth of the solution domain Ω (see Fig. 4). So the corresponding division is given in Fig. 5 where the common boundary is a semicircle l_{R^*} ($r = R^*$, $0 \leqslant \theta \leqslant \pi$).

Let M and N be the numbers of elements on the sections $\overline{AO}$ and $\overline{OG}$ in Fig. 5, and $M = N = 2$ for the case of Fig. 5. Also let $4M$ be the number of elements along the common boundary l_{R^*}. Then

$$h = O(1/M). \tag{5.2}$$

The nonconforming combinations (3.4) are used for solving this interface problem with the admissible functions (3.1), where $R = \frac{1}{2}$. Because the model is symmetric to the axis $\theta = 0$, we only need the symmetric functions $\phi_{\mu_i}(\theta)$: Kellogg's

TABLE I

Error Norms and Condition Numbers by the Nonconforming Combination for $p^- = 1$, $p^+ = 0.2$, $R = 0.5$, $R^* = 0.25$, and $M = N = 2$ While Increasing $L + 1$

$L+1$	$\|\varepsilon^+\|_{\infty, l_{R^*}}$	$\|\varepsilon^+\|_{0, l_{R^*}}$	$\|\varepsilon\|_{0,\Omega}$	$\|\varepsilon\|_h$	Con. Num.
2	0.1748×10^{-1}	0.4181×10^{-2}	0.2063×10^{-2}	0.2554×10^{-1}	105.8
3	0.2315×10^{-2}	0.6137×10^{-2}	0.8004×10^{-3}	0.1852×10^{-1}	106.3
4	0.9951×10^{-3}	0.3595×10^{-3}	0.7770×10^{-3}	0.1824×10^{-1}	106.4
5	0.1287×10^{-2}	0.4421×10^{-3}	0.7661×10^{-3}	0.1813×10^{-1}	203.3
6	0.1302×10^{-2}	0.4416×10^{-3}	0.7665×10^{-3}	0.1813×10^{-1}	203.3
8	0.1228×10^{-2}	0.4454×10^{-3}	0.7647×10^{-3}	0.1812×10^{-1}	2512
10	0.1212×10^{-2}	0.4450×10^{-3}	0.7646×10^{-3}	0.1812×10^{-1}	30485
12	0.1220×10^{-2}	0.4442×10^{-3}	0.7644×10^{-3}	0.1812×10^{-1}	0.7836×10^{6}
14	0.1470×10^{-2}	0.4394×10^{-3}	0.7628×10^{-3}	0.1813×10^{-1}	0.9098×10^{7}
16	0.1629×10^{-1}	0.3299×10^{-2}	0.1042×10^{-2}	0.2784×10^{-1}	0.1807×10^{9}

TABLE II

Calculated Coefficients for $p^{-}=1$, $p^{+}=0.2$, $R=0.5$, $R^{*}=0.25$, and $M=N=2$ While Increasing $L+1$

$L+1$	$\tilde{D}_0$	$\tilde{D}_1$	$\tilde{D}_2$	$\tilde{D}_3$	$\tilde{D}_5$	$\tilde{D}_7$	$\tilde{D}_{11}$	$\tilde{D}_{15}$
2	0.7025682	−0.1134225						
3	0.7011252	−0.1141879	−0.0127969					
4	0.7010658	−0.1141826	−0.0127701	0.0064463				
5	0.7010969	−0.1141702	−0.0127712	0.0064278				
6	0.7010966	−0.1141709	−0.0127715	0.0064263	0.0006073			
8	0.7010952	−0.1141706	−0.0127764	0.0064358	0.0006338	−0.0064830		
10	0.7010951	−0.1141705	−0.0127764	0.0064379	0.0006399	−0.0063869		
12	0.7010949	−0.1141707	−0.0127773	0.0064376	0.0005090	−0.0043917	0.0186908	
14	0.7010930	−0.1141688	−0.0127750	0.0056077	0.0005011	−0.0044549	0.0183985	
16	0.6987982	−0.1112069	−0.0119310	0.0055735	0.0006049	−0.0042872	0.0222126	−126.4932
True Coefficients [15]	0.7006584	−0.1147786	−0.0128943	0.0057785	0.0004847	0.0000406	0.0000024	0.0000002

functions (2.4) with (2.16) and the additional functions (2.18) and (2.19). In terms of true coefficients D_i ($i=0, 1, ..., 25$) given by the boundary methods [15, 16], we can compute true errors of numerical solutions obtained.

Besides, in order to discuss the stability of the nonconforming combinations, we evaluate condition numbers of the coefficient matrix T in (3.6):

$$\text{Con. Num.} = \frac{\lambda_{\max}(T)}{\lambda_{\min}(T)}, \tag{5.3}$$

where $\lambda_{\max}(T)$ and $\lambda_{\min}(T)$ are the maximal and minimal eigenvalues of T, respectively. A theoretical analysis on the condition numbers has been done in Li [14, 15]; but this paper will first provide their numerical experiments.

We shall analyze true errors of numerical solutions and condition numbers in the following four aspects. In the first three aspects, we let $p^- = 1$ and $p^+ = 0.2$ as in Strang and Fix [19] where the constant is $\alpha^* = 0.7836531$ from (2.17). In the fourth aspect, we shall change the values of p^+ while $p^- = 1$.

1. For the division in Fig. 5 where $R^* = \frac{1}{4}$ and $M = N = 2$, we have calculated error norms and condition numbers shown in Table I, while $(L+1)$ increases. All numerical results given in this section are, with double precision, calculated by a computer of the University of Toronto. For data in tables of the error norms $\|\varepsilon\|_{0,\Omega}$, $\|\varepsilon^+\|_{0,l_{R^*}}$, *et al.*, the solution domain Ω is regarded as in Fig. 5 (i.e., one eighth of that in Fig. 2), and l_{R^*} is a semi-circle ($r = R^*$, $0 \leqslant \theta \leqslant \pi$).

It is seen from Table I that the differences of the error norms $\|\varepsilon\|_h$ are very slight when $4 \leqslant L+1 \leqslant 12$, and that the condition numbers are small when $L+1 \leqslant 6$. We notice that when $L+1$ increases, the condition numbers increase very quickly. Therefore, the total number of particular solutions must be chosen small, more

TABLE III

Error Norms and Condition Numbers by the Nonconforming Combinations for $p^- = 1$, $p^+ = 0.2$, $R = 0.5$, and $R^* = 0.25$

Division	$\|\varepsilon^+\|_{\infty,l_{R^*}}$	$\|\varepsilon^+\|_{0,l_{R^*}}$	$\|\varepsilon\|_{0,\Omega}$	$\|\varepsilon\|_h$	Con. Num.
$N=M=2$, $L+1=4$	0.9951×10^{-3}	0.3595×10^{-3}	0.7770×10^{-3}	0.1824×10^{-1}	106.4
$N=M=3$, $L+1=5$	0.5814×10^{-3}	0.1985×10^{-3}	0.3363×10^{-3}	0.1202×10^{-1}	243.9
$N=M=4$, $L+1=5$	0.3358×10^{-3}	0.1132×10^{-3}	0.1914×10^{-3}	0.9007×10^{-1}	455.3
$N=M=6$, $L+1=6$	0.1588×10^{-3}	0.5030×10^{-4}	0.9203×10^{-4}	0.6020×10^{-2}	1152
$N=M=8$, $L+1=6$	0.8883×10^{-4}	0.2841×10^{-4}	0.5047×10^{-4}	0.4537×10^{-2}	2518

importantly from the stability's point of view. A comparison of approximate coefficients with true coefficients in [15] has also been made in Table II.

2. Let the division of Ω_1 in Fig. 5 be finer by increasing the numbers M and N, i.e., by decreasing h. On the basis of the coupling relation (4.37), we may increase one more particular solution in Ω_2, while the numbers M and N of divisions increase to their doubles. For example, considering that $L+1=4$ is a good choice for $M=N=2$ because of a minimal calculation work and a small condition number (see Table I), we can simply choose $L+1=5$ for $M=N=4$, and $L+1=6$ for $M=N=8$. The error norms and condition numbers have been calculated and shown in Table III, while the number M increases with $N=M$. The curves of error norms and condition numbers versus M $(=N)$ have been depicted in Figs. 6–8.

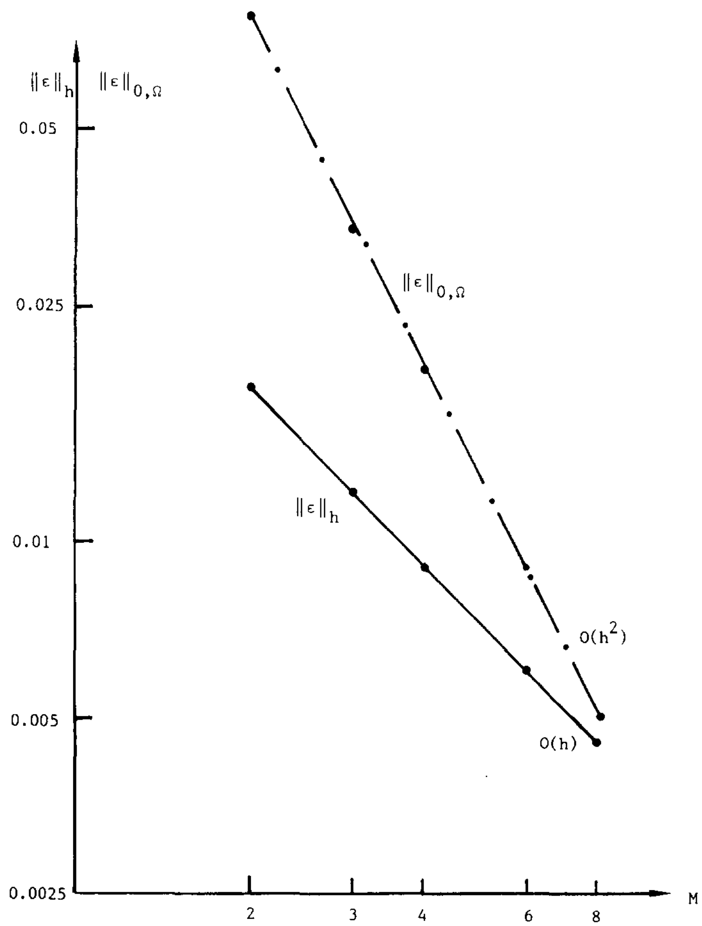

FIG. 6. The curves of the error norms, $\|\varepsilon\|_h$ and $\|\varepsilon\|_{0,\Omega}$, vs M with $N=M$.

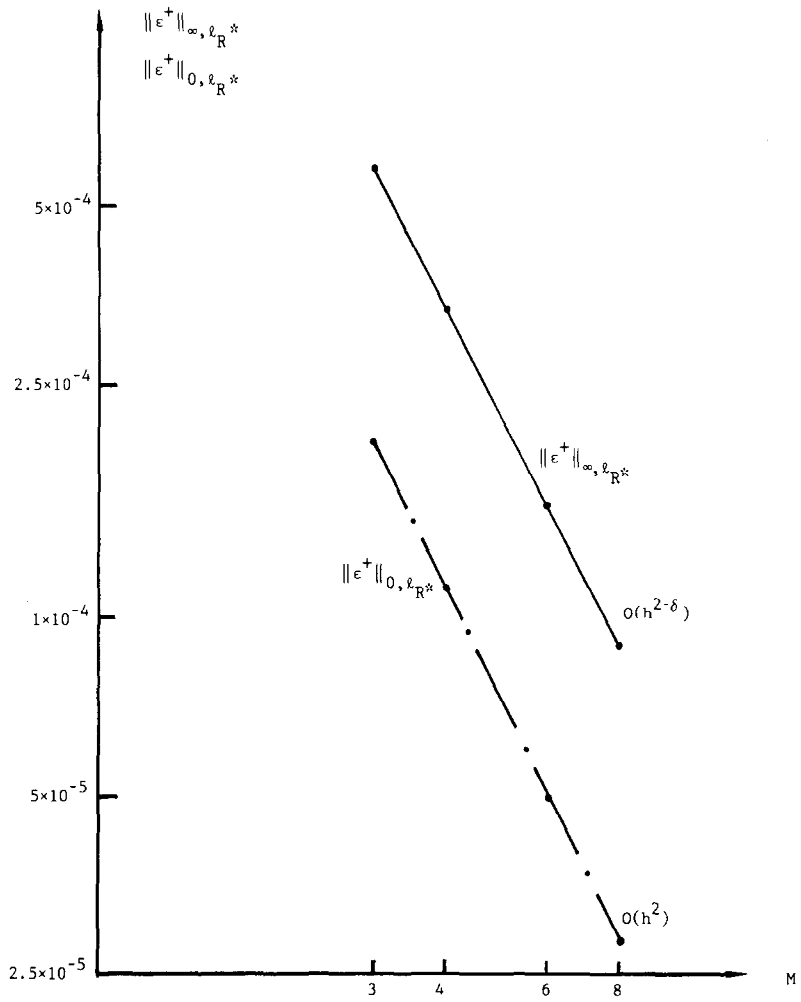

FIG. 7. The curves of the error norms, $\|\varepsilon^+\|_{0,l_{R^*}}$ and $\|\varepsilon^+\|_{\infty,l_{R^*}}$, vs M with $N = M$.

Since $h = O(1/M)$, we can see from Figs. 6–8 that the error norms and condition numbers satisfy asymptotic formulae:

$$\|\varepsilon\|_h = O(h), \tag{5.4}$$

$$\|\varepsilon\|_{0,\Omega} = O(h^2), \tag{5.5}$$

$$\|\varepsilon^+\|_{0,l_{R^*}} = O(h^2), \tag{5.6}$$

$$\|\varepsilon^+\|_{\infty,l_{R^*}} = O(h^{2-\delta}), \tag{5.7}$$

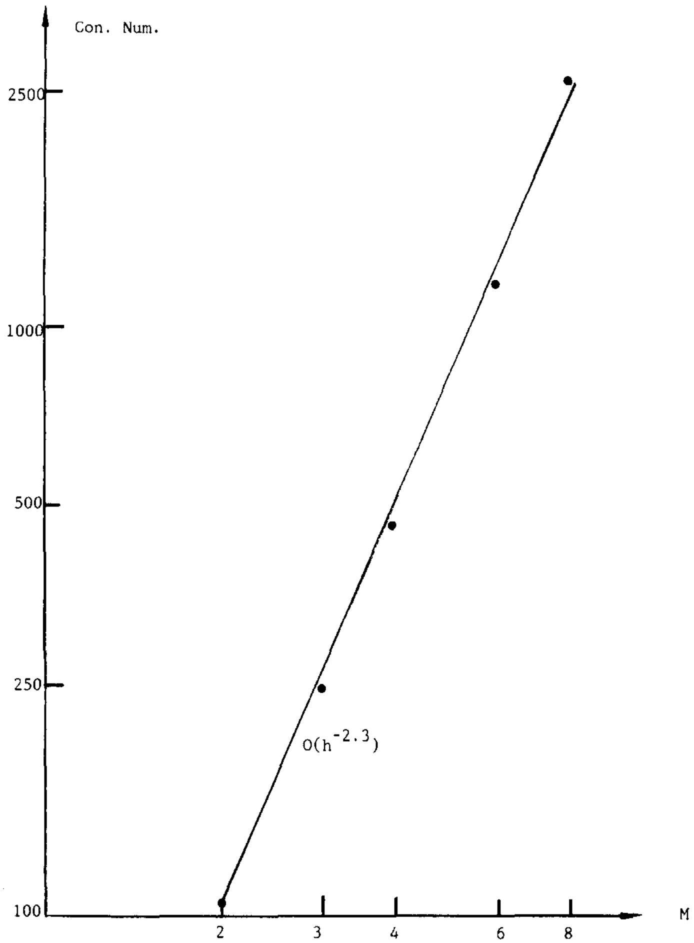

FIG. 8. The curve of the condition numbers vs M with $N = M$.

and

$$\text{Con. Num} = O(h^{-2.3}), \tag{5.8}$$

where $\varepsilon = u - u_h^*$, $\varepsilon^+ = \varepsilon|_{\Omega_2}$, and δ is an arbitrarily small positive number.

Clearly, the asymptotic formulas (5.4)–(5.7) are the same as those in the finite element method [2, 3, 5, 6, 17, 19]. Moreover, the asymptotic expression (5.4) coincides with the corollary in Section 4 concerning the coupling strategy. Equations (5.6) and (5.7) also imply that the errors of numerical solutions are small even on l_{R^*} where the admissible functions are not always continuous.

Equation (5.8) shows that when $h \to 0$, the condition numbers of T increase a

TABLE IV

Calculated Coefficients by the Nonconforming Combination for $p^- = 1$, $p^+ = 0.2$, $R = 0.5$, and $R^* = 0.25$

$M\,(=N)$	$L+1$	$\tilde{D}_0$	$\tilde{D}_1$	$\tilde{D}_2$	$\tilde{D}_3$	$\tilde{D}_4$
2	4	0.7010658	−0.1141826	−0.0127701	0.0064463	—
3	5	0.7008395	−0.1144877	−0.0128381	0.0060110	−0.0074590
4	5	0.7007581	−0.1146103	−0.0128630	0.0058936	−0.0055113
6	6	0.7007021	−0.1147023	−0.0128808	0.0058239	−0.0041104
8	6	0.7006829	−0.1147354	−0.0128868	0.0058025	−0.0036160
True coefficients [15]		0.7006584	−0.1147786	−0.0128943	0.0057785	−0.0029746

little faster than $O(h^{-2})$ in the standard finite element method [19]. Therefore, the stability of the nonconforming combinations are almost as good as that of the finite element method if the coupling strategy in this paper is employed.

In addition, we have computed the errors of calculated coefficients in Table IV. Denote

$$\delta D_l = |\tilde{D}_l - D_l|, \qquad l = 0, 1, 2, 3, \tag{5.9}$$

and depict their error curves in Fig. 9. It appears to exist asymptotic relations

$$\delta D_0 = O(h^2), \qquad \delta D_1 = O(h^2). \tag{5.10}$$

It is noteworthy that only the six basis functions in Ω_2 are required for coupling the finest division in $\hat{\Omega}_1^h$, i.e., $M = 8$. The first two basis functions of u in Ω_2 are given by

$$u \approx \tilde{D}_0 \frac{I_0(r)}{I_0(R)} + \tilde{D}_1 \frac{I_{\alpha^*}(r)}{I_{\alpha^*}(R)} \phi_{\alpha^*}(\theta) + \cdots, \qquad r \leqslant R = \tfrac{1}{2}, \tag{5.11}$$

where $\alpha^* = 0.7836531$. The values of $\tilde{D}_0$ and $\tilde{D}_1$ are obtained,

$$\tilde{D}_0 = 0.7006829, \qquad \tilde{D}_1 = -0.1147354,$$

with small relative errors 0.000035 and 0.0004, respectively. The second coefficient $\tilde{D}_1$ is more important because the corresponding basis function

$$\tilde{D}_1 \frac{I_{\alpha^*}(r)}{I_{\alpha^*}(R)} \phi_{\alpha^*}(\theta)$$

is a principal part of the singular solutions, with $u \approx O((r/R)^{0.78})$ as $r \to 0$.

3. Calculations have been done for increasing the radius R^* of the singular domain Ω_2, shown in Table V. When $R^* \to R$ $(=\tfrac{1}{2})$, the values of $\|\varepsilon\|_h$ decrease a

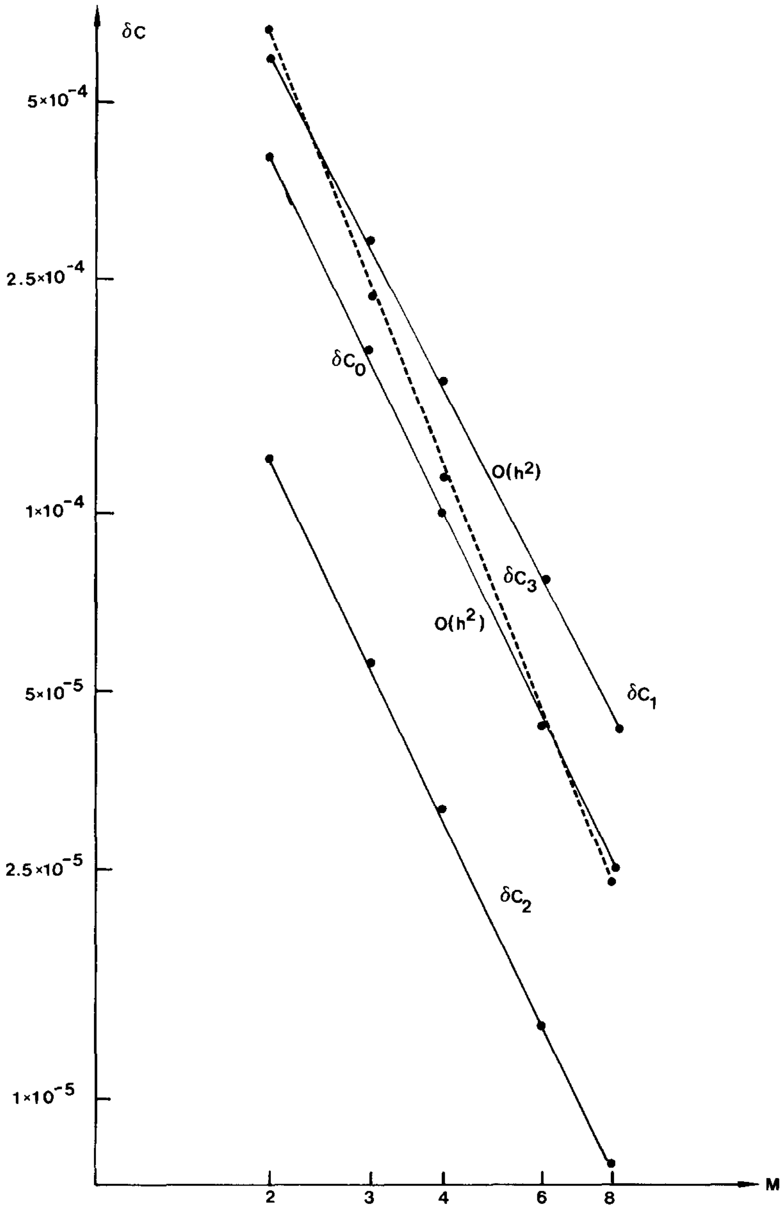

FIG. 9. The curves of relative errors of calculated coefficients vs M with $N = M$.

TABLE V

Error Norms and Condition Numbers for $p^- = 1$, $p^+ = 0.2$, $R = 0.5$, and $N = 4$ While Increasing R^*

Divisions	$\|\varepsilon^+\|_{\infty, l_{R^*}}$	$\|\varepsilon^+\|_{0, l_{R^*}}$	$\|\varepsilon\|_{0,\Omega}$	$\|\varepsilon\|_h$	Con. Num.	Unknown Num.
$R^* = 0.25$ $M = 4, L+1 = 5$	0.3358×10^{-3}	0.1132×10^{-3}	0.1914×10^{-3}	0.9007×10^{-2}	455.3	64
$R^* = 0.3125$ $M = 3, L+1 = 6$	0.3873×10^{-3}	0.1113×10^{-3}	0.1874×10^{-3}	0.9081×10^{-2}	394.8	48
$R^* = 0.375$ $M = 2, L+1 = 6$	0.5751×10^{-3}	0.1598×10^{-3}	0.2217×10^{-3}	0.9603×10^{-2}	508.6	31
$R^* = 0.4375$ $M = 2, L+1 = 6$	0.5103×10^{-3}	0.1402×10^{-3}	0.1443×10^{-3}	0.7323×10^{-2}	1276	31
$R^* = 0.475$ $M = 2, L+1 = 7$	0.4351×10^{-3}	0.1483×10^{-3}	0.1273×10^{-3}	0.6195×10^{-2}	3659	32

TABLE VI

Error Norms and Condition Numbers When $R = 0.5$, $R^* = 0.25$, $L+1 = 5$, $M = N = 4$ and $p^- = 1$ for Different p^+

p^+	$\|\varepsilon^+\|_{\infty, l_{R^*}}$	$\|\varepsilon^+\|_{0, l_{R^*}}$	$\|\varepsilon\|_{0,\Omega}$	$\|\varepsilon\|_h$	Con. Num.
100	0.3071×10^{-3}	0.1298×10^{-2}	0.2772×10^{-2}	0.1279	13184
10	0.2973×10^{-3}	0.4103×10^{-3}	0.8800×10^{-3}	0.4073×10^{-1}	1275
1	0.2782×10^{-3}	0.1432×10^{-3}	0.2972×10^{-3}	0.1409×10^{-1}	315
0.2	0.3558×10^{-3}	0.1132×10^{-3}	0.1914×10^{-3}	0.9007×10^{-2}	455
0.04	0.4079×10^{-3}	0.8904×10^{-4}	0.1181×10^{-3}	0.6525×10^{-2}	2491
0.008	0.6484×10^{-3}	0.3905×10^{-4}	0.5277×10^{-4}	0.3631×10^{-2}	31628

TABLE VII

Calculated Coefficients When $R = 0.5$, $R^* = 0.25$, $L+1 = 5$, $M = N = 4$, and $p^- = 1$ for Different p^+

p^+	α^*	$\tilde{D}_0$	$\tilde{D}_1$	$\tilde{D}_2$	$\tilde{D}_3$	$\tilde{D}_4$
100	1.3260788	0.9597324	−0.0917904	−0.0722960	0.0495255	−0.0077871
10	1.2683082	0.9546098	−0.0973639	−0.0601767	0.0404860	−0.0076972
1	1.0	0.9011589	−0.1182058	−0.0277571	0.0160052	−0.0070652
0.2	0.7836531	0.7007582	−0.1146103	−0.0128630	0.0058936	−0.0051131
0.04	0.6945953	0.3224818	−0.0586203	−0.0047703	0.0019269	−0.0026008
0.008	0.6724856	0.0867451	−0.0162162	−0.0012146	0.0004748	−0.0007068

TABLE VIII

Relative Errors $\delta C_i = (D_i/\tilde{D}_i - 1)$ with $R = 0.5$, $R^* = 0.25$, $L+1=5$, $M=N=4$, $p^- = 1$, and Different p^+, Where the Coefficients D_i as [15]

p^+	δC_0	δC_1	δC_2	δC_3	δC_4
100	0.0000560	0.000769	−0.000651	0.01788	0.8077
10	0.0000521	0.000185	−0.000818	0.01980	0.8162
1	0.0000444	−0.001237	−0.001719	0.02708	0.8565
0.2	0.0001424	−0.001466	−0.002429	0.01991	0.8528
0.04	0.0004026	−0.001196	−0.002492	0.004806	0.8181
0.008	0.0005725	−0.001011	−0.002399	−0.000998	0.8046

little; but the values of Con. Num. increase substantially. Then, we may choose a properly larger radius R^* (e.g., $R^* = 0.375$) than $R^* = 0.25$ for saving calculation work.

4. We have also investigated the influence of different p^+ upon error norms, coefficient errors and condition numbers, and shown in Tables VI–VIII.

It can be found from Table VI that the condition number is smallest at $p^+ = p^- = 1$, the case without singularity, and that the condition number is large when p^+ is either large or small.

Another interesting fact is shown in Table VI that the error norms $\|\varepsilon\|_h$ *et al.* for $p^+ > p^-$ are larger than those for $p^+ < p^-$. Also the larger p^+ is, the larger the error norms $\|\varepsilon\|_h$ *et al.* are. We notice that when $p^+ > p^-$, the value $\alpha^* > 1$ holds true for the symmetric eigenfunctions. So $u \in H^2(\Omega)$, and the finite element method using the space of piecewise linear functions is still available for the whole solution domain Ω because a good approximate solution with the error norms $\|\varepsilon\|_{1,\Omega} = O(h)$ can also be obtained.

However, when $p^+ < p^-$, the value $\alpha^* < 1$ results from (2.17). Hence the linear element method has a reduced convergence rate in solving the model problem (2.1). It is just in the case $p^+ < p^-$ that the error norms of solutions by combinations are even smaller (see Table VI). Consequently, we recommend that the nonconforming combination of Ritz–Galerkin and finite element methods with the coupling strategy (4.32) be used for the model interface problem (2.1) in Fig. 2 when $p^+ < p^-$, and for other interface problems when the conventional finite element method or finite difference method has a reduced convergence rate.

Acknowledgments

This work was supported in part by the Natural Sciences and Engineering Research Council of Canada, and by Centre de recherche informatique de Montréal Inc., the Departments of Mathematics, Applied Mathematics, and Computer Science, University of Toronto, and Department of Computer Science, Concordia University. Also I wish to express my gratitude to referees' valuable suggestions.

REFERENCES

1. I. BABUŠKA, "Solution of Problem with Interface and Singularities," in *Mathematical Aspects of Finite Elements in Partial Differential Equations*, edited by C. Boor (Academic Press, New York, 1974), p. 213.
2. I. BABUŠKA AND A. K. AZIZ, "Survey Lectures on the Mathematical Foundations of the Finite Element Method," *The Mathematical Foundations of the Finite Element Method with Application to Partial Differential Equations*, edited by A. K. Aziz, (Academic Press, New York, London, 1972), p. 3.
3. K. J. BATH AND E. L. WILSON, *Numerical Methods in Finite Element Analysis* (Prentice–Hall, Englewood Cliffs, NJ 1976).
4. G. BIRKHOFF, *J. Approx. Theory* **6**, 215 (1972).
5. G. BIRKHOFF AND R. E. LYNCH, *Numerical Solution of Elliptic Problems* (SIAM, Philadelphia, 1984).
6. P. G. CIARLET, *The Finite Element Method for Elliptic Problem* (North–Holland, Amsterdam, New York, 1978).
7. G. J. FIX, S. GULATI, AND G. I. WAKOFF, *J. Comput. Phys.* **13**, 209 (1973).
8. J. A. GREGORY, D. FISHELOV, B. SCHIFF, AND J. R. WHITEMAN, *J. Comput. Phys.* **29**, 133 (1978).
9. H. HAN, *Numer. Math.* **30**, 39 (1982).
10. R. B. KELLOGG, "Singularities in Interface Problem," in *Numerical Solution of Partial Differential Equations* II, edited by B. Hubbard (Academic Press, New York, 1971), p. 351.
11. R. B. KELLOGG, "Higher Order Singularities for Interface Problems," in *The Mathematical Foundations of the Finite Element Method with Application to Partial Differential Equations*, edited by A. K. Aziz, (Academic Press, New York, London, 1972), p. 589.
12. R. B. KELLOGG, *Appl. Anal.* **4** 101 (1975).
13. Z. C. LI, *J. Approx. Theory* **39**, 132 (1983).
14. Z. C. LI, *Numer. Math.* **49**, 475 (1986).
15. Z. C. LI, Ph.D. thesis, University of Toronto, May 1986, winner of the 1987 Dissertation Award of CAMS/SCMA (unpublished).
16. Z. C. LI, R. MATHON, AND P. SERMER, *SIAM J. Numer. Anal.* **24** 487 (1987).
17. R. SCOTT, *Math. Comput.* **30**, 681 (1976).
18. S. L. SOBOLEV, *Application of Functional Analysis in Mathematical Physics*, (AMS, Providence, R. I., 1963).
19. G. STRANG AND G. J. FIX, *An Analysis of the Finite Element Method* (Prentice–Hall, Englewood Cliffs, NJ, 1973).
20. R. W. THATCHER, *Numer. Math.* **25**, 163 (1976).
21. J. R. WHITEMAN AND N. PAPMICHAEL, *ZAMP* **23**, 665 (1972).
22. G. N. WATSON, A Treatise on the Theory of Bessel Functions, 2nd ed. (Cambridge Univ. Press, London/New York, 1944).
23. N. M. WIGLEY, *Math. Comput.* **23**, 395 (1969).
24. N. M. WIGLEY, *J. Comput. Phys.* **78**, 369 (1988).
25. A. P. ZIELINSKI AND O. C. ZIENKIEWICZ, *Int. J. Numer. Methods Eng.* **21**, 509 (1985).
26. O. C. ZIENKIEWICZ, D. M. KELLEY, AND P. BETTESS, *Int. J. Numer. Methods Eng.* **11**, 335 (1977).